Lecture No. One

Signals and Systems II

By

Assist. Prof. Dr.

Yousif Ismail Al Mashhadnay

2019 – 2020

No	Subject	Week (4 H/W)
1.	**Ch. 9. Sampling and Quantization** 9.1. Introduction. 9.2. Ideal impulse-train sampling. 9.3. Reconstruction of a band-limited signal from its samples. 9.4. Zero-order hold. 9.5. Quantization (uniform and non-uniform). 9.6. Solved Problem.	2
2.	**Ch. 10. Time-domain analysis of discrete-time systems** 10.1. Introduction. 10.2. Finite-difference equation representation of LTID systems 10.3. Representation of sequences using Dirac delta functions 10.4. Impulse response of a system	3

	10.5. Convolution sum *10.6. Graphical method for evaluating the convolution sum* *10.7. Properties of the convolution sum*	
3.	***Ch. 11. Discrete-time Fourier Series and Transform*** *11.1. Introduction.* *11.2. Discrete-time Fourier series* *11.3. Periodicity of DTFS coefficients* *11.4. Fourier transform for aperiodic functions* *11.5. Existence of the DTFT* *11.6. DTFT of periodic functions* *11.7. Properties of the DTFT and the DTFS* *11.8. Frequency response of LTID systems* *11.9. Magnitude and phase spectra* *11.10. Continuous- and discrete-time Fourier transforms*	**3**

References:

1) *"Continuous and Discrete Time Signals and Systems" , 2007 ; By: Mrinal Mandal and Amir Asif*

2) *"Signals and Systems" 2008, By : Steven T. Karris*

Important Symbols

Symbol	*Detail*
CT	continuous-time
DT	discrete-time
LTI	linear time-invariant
LTIC	linear time-invariant continuous-time
CTFS	continuous-time Fourier series
CTFT	continuous-time Fourier transform
LTID	linear time-invariant discrete-time
DTFS	discrete-time Fourier series
DTFT	discrete-time Fourier transform
DFT	discrete Fourier transform
FIR	finite impulse response
IIR	infinite impulse response
ROC	Region of Convergence

Symbol	*Detail*
CCD	charge coupled device
1D	one-dimensional
2D ND	two-dimensional ; and so … N-dimensional
SISO	single inputs and single outputs
MIMO	multiple inputs and multiple outputs
GPA	grade point average
A/D	Analogue to Digital
D/A	Digital to Analogue
LPF	Low pass filter
BPF	Band pass filter
DSP	digital signal processing
FFT	fast Fourier transform
LT	Laplace transform

Sampling and Quantization

This chapter presents the following items as follow:

9.1. Introduction.

9.2. Ideal impulse-train sampling.

9.3. Reconstruction of a band-limited signal from its samples.

9.4. Zero-order hold.

9.5. Quantization (uniform and non-uniform).

9.6. Solved Problem.

Sampling and Quantization

9.1. Introduction

Part I of the study year covered techniques for the analysis of continuous-time (CT) signals and systems. In Part II, we consider the corresponding analysis tech-niques for discrete-time (DT) sequences and systems. A DT sequence may occur naturally. Examples are the one-dimensional (1D) hourly measurements $x[k]$ made with an electronic thermometer, or the two-dimensional (2D) image $x[m, n]$ recorded with a digital camera, as illustrated earlier in Fig. 1.1. Alter-natively, a DT sequence may be derived from a CT signal by a process known as sampling. A widely used procedure for processing CT signals consists of trans-forming these signals into DT sequences by sampling, processing the resulting DT sequences with DT systems, and converting the DT outputs back into the CT domain. This concept of DT processing of CT signals is illustrated by the schematic diagram shown in Fig. 9.1. Here, the input CT signal $x(t)$ is con-verted to a DT sequence $x[k]$ by the *sampling* module, also referred to as the A/D converter. The DT sequence is then processed by the *DT system* module. Finally, the output $y[k]$ of the DT module is converted back into the CT domain by the *reconstruction* module. The reconstruction module is also referred to as the D/A converter. Although the intermediate waveforms, $x[k]$ and $y[k]$, are DT sequences, the overall shaded block may be considered as a CT system since it accepts a CT signal $x(t)$ at its input and produces a CT output $y(t)$. If the internal working of the shaded block is hidden, one would interpret that the overall operation of Fig. 9.1 results from a CT system.

In practice, a CT signal can either be processed by using a full CT setup, in which the individual modules are themselves CT systems (as explained in the first semester), or by using a CT–DT hybrid setup (as shown in Fig. 9.1). Both approaches have advantages and disadvantages. The primary advantage of CT signal processing is its higher speed as DT systems are not as fast as their counterparts in the CT domain due to limits on the sampling rate of the A/D converter and the clock rate of the processor used to implement the DT systems. In spite of its limitation in speed, there are important advantages with DT sig-nal processing, such as improved flexibility, self-calibration, and data-logging. Whereas CT systems have a limited performance range, DT systems are more flexible and can be reprogrammed such that the same hardware can be used in a variety of different applications.

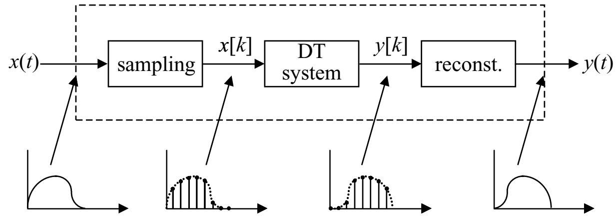

Fig. 9.1. Processing CT signals using DT systems.

In addition, the characteristics of CT systems tend to vary with changes in the operating conditions and with age. The DT systems have no such problems as the digital hardware used to implement these systems does not drift with age or with changes in the operating conditions and, therefore, can be self-calibrated easily. Digital signals, obtained by quantizing DT sequences, are less sensitive to noise and interference than analog signals and are widely used in communication systems. Finally, the data available from the DT systems can be stored in a digital server so that the performance of the system can be monitored over a long period of time. In summary, the advan-tages of the DT system outweigh their limitations in most applications. Until the late 1980s, most signal processing applications were implemented with CT systems constructed with analog components such as resistors, capacitors, and operational amplifiers. With the recent availability of cheap digital hardware, it is a common practice now to perform signal processing in the DT domain based on the hybrid setup shown in Fig. 9.1.

Although, a CT–DT hybrid setup similar to Fig. 9.1 is advantageous in many applications, care should be taken during the design stage. For example, during the sampling process some loss of information is generally inevitable. Consequently, if the system is not designed properly, the performance of a CT–DT hybrid setup may degrade significantly as compared with a CT setup. In this chapter, we focus on the analysis of the sampling process and the converse step of reconstructing a CT signal from its DT version. In addition, we also analyze the process of quantization for converting an analog signal to a digital signal. Both time-domain and frequency-domain analyses are used where appropriate.

The organization of Chapter 9 is as follows. Section 9.1 general introduction for sampling. Section 9.2 and 9.3 introduces the impulse-train sampling process and derives a necessary condition, referred to as the sampling theorem, under which a CT signal can be perfectly reconstructed from its sampled DT version. We observe that violating the sampling theorem leads to distortion or aliasing in the frequency domain. Section 9.4 introduces the practical implementations for impulse-train sampling. These implementations are referred to as pulse-train sampling and zero-order hold.

In Section 9.5, we introduce another discretization process called quantization, which, in conjunction with sampling, converts a CT signal into a digital signal.

9.2 Ideal impulse-train sampling

In this section, we consider sampling of a CT signal $x(t)$ with a bounded CTFT $X(\omega)$ such that

$$X(\omega) = 0 \quad \text{for} \quad |\omega| > 2\pi\beta. \tag{9.1}$$

A CT signal $x(t)$ satisfying Eq. (9.1) is referred to as a baseband signal, which is band-limited to $2\pi\beta$ radians/s or β Hz. In the following discussion, we prove that a baseband signal $x(t)$ can be transformed into a DT sequence $x[k]$ with no loss of information if the sampling interval T_s satisfies the criterion that $T_s \leq 1/2\beta$.

To derive the DT version of the baseband signal $x(t)$, we multiply $x(t)$ by an impulse train:

$$s(t) = \sum_{k=-\infty}^{\infty} \delta(t - kT_s), \tag{9.2}$$

where T_s denotes the separation between two consecutive impulses and is called the sampling interval. Another related parameter is the sampling rate ω_s, with units of radians/s, which is defined as follows:

$$\omega_s = \frac{2\pi}{T_s}. \tag{9.3}$$

Mathematically, the resulting sampled signal, $x_s(t) = x(t) \cdot s(t)$, is given by

$$x_s(t) = x(t) \sum_{k=-\infty}^{\infty} \delta(t - kT_s) = \sum_{k=-\infty}^{\infty} x(kT_s)\delta(t - kT_s). \tag{9.4}$$

Figure 9.2 illustrates the time-domain representation of the process of the impulse-train sampling. Figure 9.2(a) shows the time-varying waveform representing the baseband signal $x(t)$. In Figs. 9.2(b) and (c), we plot the sampled signal $x_s(t)$ for two different values of the sampling interval. In Fig. 9.2(b), the sampling interval $T_s = T$ and the sampled signal $x_s(t)$ provides a fairly good approximation of $x(t)$. In Fig. 9.2(c), the sampling interval T_s is increased to $2T$. With T_s set to a larger value, the separation between the adjacent samples in $x_s(t)$ increases. Compared to Fig. 9.2(b), the sampled signal in Fig. 9.2(c) provides a coarser representation of $x(t)$. The choice of T_s therefore determines how accurately the sampled signal $x_s(t)$ represents the original CT signal $x(t)$. To determine the optimal value of T_s, we consider the effect of sampling in the frequency domain.

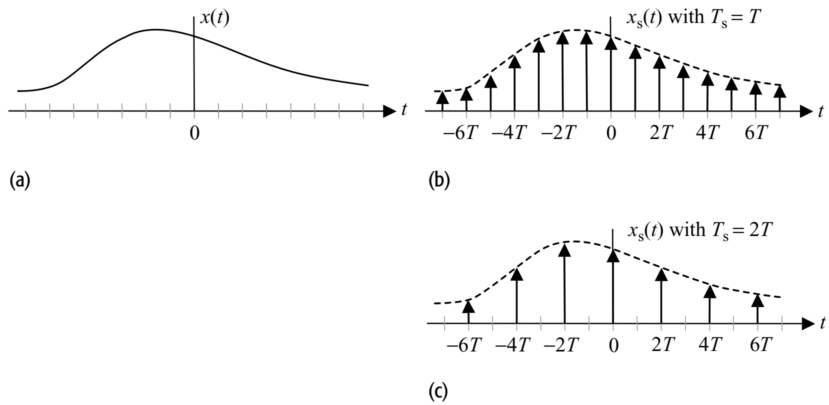

Fig. 9.2. Time-domain illustration of sampling as a product of the band-limited signal and an impulse train. (a) Original signal $x(t)$; (b) sampled signal $x_s(t)$ with sampling interval $T_s = T$; (c) sampled signal $x_s(t)$ with sampling interval $T_s = 2T$.

Calculating the CTFT of Eq. (9.4), the CTFT $X_s(\omega)$ of the sampled signal $x_s(t)$ is given by

$$X_s(\omega) = \Im\left\{x(t)\sum_{k=-\infty}^{\infty}\delta(t-kT_s)\right\} = \frac{1}{2\pi}F\{x(t)\} * \Im\left\{\sum_{k=-\infty}^{\infty}\delta(t-kT_s)\right\}$$
$$= \frac{1}{2\pi}\left[X(\omega) * \frac{2\pi}{T_s}\sum_{m=-\infty}^{\infty}\delta\left(\omega - \frac{2m\pi}{T_s}\right)\right] = \frac{1}{T_s}\sum_{m=-\infty}^{\infty}X\left(\omega - \frac{2m\pi}{T_s}\right) \tag{9.5}$$

where $*$ denotes the CT convolution operator. In deriving Eq. (9.5), we used the following CTFT pair:

$$\sum_{k=-\infty}^{\infty}\delta(t-kT_s) \overset{\text{CTFT}}{\longleftrightarrow} \frac{2\pi}{T_s}\sum_{m=-\infty}^{\infty}\delta\left(\omega - \frac{2m\pi}{T_s}\right)$$

based on entry (19) of Table 5.2. Equation (9.5) implies that the spectrum $X_s(\omega)$ of the sampled signal $x_s(t)$ is a periodic extension, consisting of the shifted replicas of the spectrum $X(\omega)$ of the original baseband signal $x(t)$. Figure 9.3 illustrates the frequency-domain interpretation of Eq. (9.5). The spectrum of the original signal $x(t)$ is assumed to be an arbitrary trapezoidal waveform and is shown in Fig. 9.3(a). The spectrum $X_s(\omega)$ of the sampled signal $x_s(t)$ is plotted

Fig. 9.3. Frequency-domain illustration of the impulse-train sampling. (a) Spectrum $X(\omega)$ of the original signal $x(t)$; (b) spectrum $X_s(\omega)$ of the sampled signal $x_s(t)$ with sampling rate $\omega_s \geq 4\pi\beta$; (c) spectrum $X_s(\omega)$ of the sampled signal $x_s(t)$ with sampling rate $\omega_s < 4\pi\beta$.

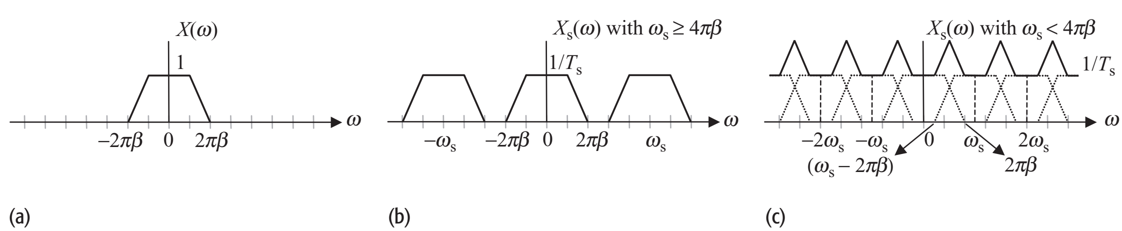

in Figs. 9.3(c) and (d) for the following two cases:

case I $\qquad \omega_s \geq 4\pi\beta$;

case II $\qquad \omega_s < 4\pi\beta$.

When the sampling rate $\omega_s \geq 4\pi\beta$, no overlap exists between consecutive replicas in $X_s(\omega)$. However, as the sampling rate ω_s is decreased such that $\omega_s < 4\pi\beta$, adjacent replicas overlap with each other. The overlapping of replicas is referred to as aliasing, which distorts the spectrum of the original baseband signal $x(t)$ such that $x(t)$ cannot be reconstructed from its samples. To prevent aliasing, the sampling rate $\omega_s \geq 4\pi\beta$. This condition is referred to as the *sampling theorem* and is stated in the following.†

Sampling theorem *A baseband signal $x(t)$, band-limited to $2\pi\beta$ radians/s, can be reconstructed accurately from its samples $x(kT)$ if the sampling rate ω_s, in radians/s, satisfies the following condition:*

$$\omega_s \geq 4\pi\beta. \tag{9.6a}$$

Alternatively, the sampling theorem may be expressed in terms of the sampling rate $f_s = \omega_s/2\pi$ in samples/s, or the sampling interval T_s. To prevent aliasing,

sampling rate (samples/s) $\qquad f_s \geq 2\beta$; (9.6b)

or

sampling interval $\qquad T_s \leq 1/2\beta$. (9.6c)

The minimum sampling rate f_s (Hz) *required for perfect reconstruction of the original band-limited signal is referred to as the* Nyquist rate.

The sampling theorem is applicable for *baseband* signals, where the signal contains low-frequency components within the range $0 - \beta$ Hz. In some applications, such as communications, we come across bandpass signals that also contain a band of frequencies, but the occupied frequency range lies within the band $\beta_2 - \beta_1$ Hz with $\beta_1 \neq 0$. In these cases, although the maximum frequency of β_2 Hz implies the Nyquist sampling rate of $2\beta_2$ Hz it is possible to achieve perfect reconstruction with a lower sampling rate (see Problem 9.8).

† The sampling theorem was known in various forms in the mathematics literature before its application in signal processing, which started much later, in the 1950s. Several people developed independently or contributed towards its development. Notable contributions, however, were made by E. T. Whittaker (1873–1956), Harry Nyquist (1889–1976), Karl Küpfmüller (1897–1977), V. A. Kotelnikov (1908–2005), Claude Shannon (1916–2001), and I. Someya.